Solid Earth Discuss., 5, 2483–2507, 2013
www.solid-earth-discuss.net/5/2483/2013/
doi:10.5194/sed-5-2483-2013

Solid Earth Discussions
Open Access

Lithosphere and upper-mantle structure of the southern Baltic Sea estimated from modelling relative sea-level data with glacial isostatic adjustment

H. Steffen[1], **G. Kaufmann**[2], **and R. Lampe**[3]

[1]Lantmäteriet, Lantmäterigatan 2c, 80182 Gävle, Sweden
[2]Freie Universität Berlin, Institut für Geologische Wissenschaften, Fachrichtung Geophysik, Malteserstr. 74–100, Haus D, 12249 Berlin, Germany
[3]Ernst-Moritz-Arndt-Universität Greifswald, Institut für Geographie und Geologie, F.-L.-Jahn-Str. 16, 17487 Greifswald, Germany

Received: 26 November 2013 – Accepted: 29 November 2013
– Published: 23 December 2013

Correspondence to: H. Steffen (holger-soren.steffen@lm.se)

Published by Copernicus Publications on behalf of the European Geosciences Union.

Lithosphere and upper-mantle structure of the southern Baltic Sea

H. Steffen et al.

Abstract

During the last glacial maximum, a large ice sheet covered Scandinavia, and the Earth's surface was depressed by several 100 m. Beyond the limit of this Fennoscandian ice sheet, mass redistribution in the upper mantle led to the development of peripheral bulges around the glaciated region. These once uplifted areas subside since the begin of deglaciation due to the viscoelastic behavior of the mantle. Parts of this subsiding region are located in northern central Europe in the coastal parts of Denmark, Germany and Poland.

We analyze relative sea-level (RSL) data of these regions to determine the lithospheric thickness and radial mantle viscosity structure for distinct regional RSL subsets. We load a one-dimensional Maxwell-viscoelastic earth model with a global ice-load history model of the last glaciation. We test two commonly used ice histories, RSES from the Australian National University and Ice-5G from the University of Toronto.

Our results indicate that the lithospheric thickness varies, depending on the ice model used, between 60 and 160 km. The lowest values are found in the Oslo Graben area and the western German Baltic Sea coast. In between, thickness increases by at least 30 km tracing the Fyn High. In Poland, lithospheric thickness values up to 160 km are reached. However, the latter values are not well constrained due to a low number of RSL data from the Polish area. Upper-mantle viscosity is found to bracket $[2–7] \times 10^{20}$ Pa s when using Ice-5G. Employing RSES much higher values of 2×10^{21} Pa s yield for the southern Baltic Sea, which suggests a revision of this ice-model version. We confirm that the lower-mantle viscosity in Fennoscandia can only be poorly resolved.

The lithospheric structure inferred partly supports structural features of regional and global lithosphere models based on thermal or seismological data. While there is agreement in eastern Europe and southwest Sweden, the structure in an area from south of Norway to northern Germany shows large discrepancies for two of the tested

models. It thus remains challenging to sufficiently determine the Fyn High as seen with seismics with the help of glacial isostatic adjustment modelling.

1 Introduction

During the last colder climatic phase with average surface temperatures being about 10 °C lower than today, northern Europe – next to other parts in the world – was covered by an extensive ice sheet. The mass of this so-called Fennoscandian ice sheet suppressed the Earth's crust into the mantle, leading to surface depressions of several hundreds of meters underneath the ice. Beyond the ice-covered area, a peripheral bulge developed around the ice sheet due to the finite strength of the elastic lithosphere. This narrow band of 100–200 km width was uplifted up to a few tens of meters (Steffen and Wu, 2011). During and after the deglaciation phase, the mass redistribution is reversed, forcing uplift of the formerly glaciated areas and subsidence of the peripheral bulge. These changes are, due to the viscoelastic and thus time-delayed behavior of the mantle, still observable today.

This dynamic response of the Earth during glacial cycles is known as glacial isostatic adjustment (GIA). There are several observation methods for this process, and Fennoscandia has turned out to be the key area for GIA studies (e.g. Steffen and Wu, 2011, and references therein). Relative sea-level (RSL) data provide the longest observational dataset from all observations, occasionally dating back several thousands of years. They document the movement of coastlines as a consequence of both the water redistribution between oceans and ice sheets and the deformation of the Earth's surface that occurred in the past. RSL data are therefore valuable in modelling the GIA process, as they can separate effects of ice history from Earth rheology. A large number of RSL data is available for Fennoscandia (e.g. Steffen and Wu, 2011, and references therein).

Other datasets, such as movements of the Earth's crust observed by the Global Positioning System (GPS), are based on modern geodetic observations. These geodetic data are very accurately measured, but they cover a much smaller time span in the decadal range, thus showing only the current rate of deformation (e.g. Wu et al., 2013). The uplift rates determined by GPS observations in the former center of glaciation in Fennoscandia are about 10 mm yr^{-1}, while much lower subsidence values of at most 2 mm yr^{-1} are determined in the bulge region (Lidberg et al., 2010).

GIA observations such as RSL and GPS data can be employed for the determination of the Earth's internal structure, in particular the lithospheric thickness and mantle viscosities (e.g. Steffen and Wu, 2011, and references therein). Often, this is done in formerly glaciated areas, e.g. Fennoscandia, the Barents Sea or the British Isles. As an example, Steffen and Kaufmann (2005) subdivided the Fennoscandian RSL dataset into RSL data located in the center around the Baltic Sea and coastal data mainly along the Norwegian coast. They found clear differences in the Earth's structure of the two regions. Vink et al. (2007) subdivided a RSL dataset of the southern North Sea into three distinct regionally subsets. A regional variation of the lithospheric thickness as well as regionally differing isostatic subsidence curves were determined.

The earth structure beneath northern Europe derived from GIA data can be summarized as follows: in Fennoscandia, the lithosphere is laterally varying with a thick root of more than 200 km in central-east Fennoscandia, becoming thinner towards the west (Steffen and Wu, 2011). Southwest Sweden is predicted to have a lithospheric thickness of about 100 km, the German North Sea coast as well as the Norwegian Atlantic coast of about 80 km (Vink et al., 2007; Steffen and Wu, 2011). Note that we refer the term lithosphere to the strong outer shell of the Earth composed of the crust and upper part of the mantle, which both have an elastic rheology.

Below the lithosphere, a zone of lower viscosity such as an asthenosphere is still under debate (Steffen and Kaufmann, 2005). The upper-mantle viscosity can be bracketed between 10^{20} and 10^{21} Pa s, whereas the latest results calculated from different data yield between [3–8] $\times 10^{20}$ Pa s. The viscosity is increasing towards the lower mantle (Steffen and Kaufmann, 2005). The lower-mantle viscosity is assumed to be around 1–2 orders of magnitude higher. Its determination, however, is complicated as the resolving power of all data in Fennoscandia is too low to resolve more accurate values for the lower mantle.

The lithosphere determined in GIA studies should be comparable to results from other studies, e.g. seismological studies. However, there are different geophysical definitions of the lithosphere depending on the method used for its determination. There are rheological, petrological, elastic, thermal, electrical and seismic definitions. It is beyond the scope of this paper to discuss all definitions in detail, the individual determination in view of the definition as well as the relation of each lithosphere to another. We therefore refer the interested reader to Tesauro et al. (2009), Eaton et al. (2009) and Artemieva (2009) for a detailed overview. But, it has been noted that some of the definitions should coincide, such as the thermal definition with the seismological one (Tesauro et al., 2009). The seismological lithosphere is generally the high-velocity outer layer of the Earth, approximately coincident with the lithosphere, which typically overlies a low velocity zone (Eaton et al., 2009). The thermal lithosphere is defined by a depth to a constant isotherm or by the depth of the intersection of a continental geotherm either with a mantle adiabat or with a temperature close to mantle solidus (Artemieva, 2009). We will see that the lithospheric structure in northern Europe as derived with GIA modelling and outlined above, is in agreement to thermal and seismological studies on the lithosphere on a broad scale, but only in terms of lateral variation and not in an exact match of thicknesses.

Gregersen et al. (2002) provided a NE-SW profile from southern Sweden to central Germany based on *P* wave velocity perturbation. The generalized profile shows a 300 km lithosphere and mesosphere northeast of the Tornquist Zone, but this value may be too thick, which is not further discussed in Gregersen et al. (2002). The lithospheric thickness then decreases to about 125 km between the Fyn High and the Tornquist Zone in Denmark, and about 80 km southwest of the Fyn High in Germany.

Tesauro et al. (2009) showed a map of thermal lithospheric thickness in Europe south of 60° N latitude. In southern Sweden, they find a thickness exceeding 180 km. The thickness is then decreasing to about 120 km in northeastern Germany. In the

SED
5, 2483–2507, 2013

southern North Sea, they find an average of about 135 km in Belgium and about 110 km in the Netherlands and northwest Germany. A comparison with receiver function data mirrored the lateral variation (Tesauro et al., 2009), and visual comparison with newer S-receiver function results (Geissler et al., 2010) supports the results as well. The British Isles have varying thicknesses between 100 and 180 km.

Hamza et al. (2012) developed a global distribution map of the thermal lithospheric thickness. In southern Sweden, lithospheric thickness is found to be between 170 and 210 km. Similar values arise for the German Baltic Sea coast and Denmark. The southern North Sea has a lithosphere of about 160 to 170 km thickness.

Recently, Priestley and McKenzie (2013) introduced a seismologically determined lithosphere model that also includes thermal information. In the southern Baltic Sea area, there are two major structural features. First, lithospheric thickness decreases from 260 km in the east to 110–120 km in the west. The gradient is almost constant, but slightly steeper in southwestern Sweden. Second, from western central Denmark towards the North Sea, an area enveloping the Fyn High, lithospheric thickness remains at an almost constant level of about 140 km. To the north and south it drops to about 110 km.

The purpose of this study is to determine the Earth's structure underneath the southern Baltic Sea with special attention given to the lateral variation of the lithosphere. We use RSL data that emerged mainly in the last years. They are subdivided in regional subsets similar to the studies by Lambeck et al. (1998) and Vink et al. (2007) to derive radial profiles of the Earth for 5 different regions of the southern Baltic Sea. The best-fitting models allow us to estimate the isostatic contribution in each region, to highlight the lateral structure and to describe the peripheral bulge in northern Central Europe. We also compare the lithospheric thickness as derived in regional subsets to three lithospheric thickness models available to us.

In the next Sect. 2, we will describe the RSL data used. This is followed by an overview of the modelling technique and the ice models implemented in this study (Sect. 3). Results are presented in Sect. 4 and discussed in Sect. 5. This includes

SED
5, 2483–2507, 2013

a comparison to lithosphere models available to us. Finally, we summarize our main findings in Sect. 6.

2 Relative sea-level data

In the past decades mostly basal peat layers (sensu Lange and Menke, 1967) found in sediment cores were used to reconstruct the postglacial sea-level rise along the southern and western Baltic coast. However, these sea-level index points, often scattered over larger areas, may have experienced different vertical movements due to isostasy and/or compaction and thus are compromised by large uncertainties in many respects. More recently, new sampling, positioning and dating techniques allowed the detection of archaeological underwater finds such as settlement refuse, boats, fish weirs and fire places, or drowned in-situ tree stumps (Tauber, 2007; Lübke et al., 2011). Such finds provide numerous samples for a distinct site and a specific elevation relative to modern sea level. Other approaches use a set of isolation basins or coastal mires to trace the sea-level variation over a longer period in a very limited area (Yu et al., 2004; Lampe et al., 2011). Such investigations allow the construction of sea-level curves owing to better resolution and minor altitude errors and thus higher precision. They provide an excellent base to test different ice-load history models and earth models as well.

For this study we use published datasets from Denmark (Great Belt and Halsskov Fjord: Christensen et al., 1997), northeastern Germany (Schleswig-Holstein: Winn et al., 1986; Jakobsen, 2004; Mecklenburg-Vorpommern: Lampe et al., 2007; Hoffmann et al., 2009), Poland (Uścinowicz, 2003) and a few data from Lithuania (Curonian Lagoon and adjacent areas: Bitinas et al., 2000, 2002). We group these data into three regional subsets: west of Darss Peninsula with 65 index points, Fyn, Darss Peninsula and Rügen Island with 133 index point, and Poland and Lithuania with 31 index points (Fig. 1).

A common feature of the investigated regions is that the postglacial sea-level rise started not before the transgressing ocean inundated the Danish Great Belt and in-

SED
5, 2483–2507, 2013

vaded the Baltic basin. Age determinations of the earliest marine influence in the southern Baltic lie between 9.4 and 8.0 ka cal BP (Hofmann and Winn, 2000; Rößler et al., 2009; Bennike et al., 2004). Because the threshold depth of the Great Belt amounts to 25 m below sea level, the sea-level change cannot be traced to greater depths. In coastal regions the Pleistocene relief further restricts the depth where the former sea level can be determined.

Therefore, the lowest sea-level index points used in the study come from offshore areas in the Great Belt and Kiel Bight, while all other points are from near coastal on- and offshore areas that are located in much lesser depths. Mostly, the data used belong to larger datasets but are evaluated as most reliable, considering dated material, sedimentary facies and age-depth relations.

In addition to these new data for the southern Baltic Sea coast, we investigate two sub-regional datasets from the Fennoscandian RSL data used in Steffen and Kaufmann (2005). The first covers the Oslo Graben and surrounding. It contains 77 data from northern Denmark and the Oslo Fjord. The second subset includes 44 data from southwest Sweden. In addition, 12 archaeological data from dated Hensbacka sites around the city of Gothenburg as described and used in Schmitt et al. (2009) are added resulting in a total of 56 data for this dataset.

Figure 1 shows the spatial and temporal distribution of the datasets. One can clearly distinguish the characteristics of each dataset. SW Sweden and the northern samples of the Oslo Graben RSL data highlight land uplift over the last 15 000 yr and thus are typical examples of near-field data. The Danish samples as well as the other datasets trace the sea-level rise in the last 12 000 yr, here in conjunction with isostatic subsidence of the forebulge, and therefore illustrate the typical behavior of far-field data. We also see that the vertical range of near-field data, here more than 200 m, is much larger than that of the far-field data, having less than 30 m. The main sea-level change visible in the latter data happens before 7 ka BP. After that, the change is in the meter range.

3 Modelling

3.1 Earth models

The modelling is undertaken with the software package ICEAGE (Kaufmann, 2004), which was successfully used in earlier GIA studies (e.g. Steffen and Kaufmann, 2005; Vink et al., 2007; Steffen et al., 2010). We briefly summarize the main characteristics and methods only, and refer the reader to Steffen and Kaufmann (2005) for more information.

We employ a spherically symmetric (one-dimensional), compressible, Maxwell-viscoelastic earth model having three layers to be varied; lithospheric thickness, upper- and lower-mantle viscosity. An inviscid Earth's core is set as lower boundary. The viscosity is kept constant within a layer. Elastic parameters are taken from the Preliminary Reference Earth Model (Dziewonski and Anderson, 1981, PREM). Lithospheric thickness is varied between 60 and 160 km, upper-mantle viscosity between 10^{19} and 4×10^{21} Pa s, and lower-mantle viscosity between 10^{21} and 10^{23} Pa s. Based on former investigations (e.g. Steffen and Kaufmann, 2005; Vink et al., 2007) these values cover plausible values for three-layer models well.

We follow the pseudo-spectral approach described in Mitrovica et al. (1994) and Mitrovica and Milne (1998) for the calculation of relative sea levels with our models. It is an iterative procedure in the spectral domain with a spherical harmonic expansion up to degree 192, which solves the sea-level equation (Farrell and Clark, 1976) for a rotating Earth. Relative sea levels are calculated for 1089 (11 × 11 × 9) different so-called three-layer earth models which are then compared to our regional RSL datasets based on a least-squares misfit

$$\chi = \sqrt{\frac{1}{n}\sum_{i=1}^{n}\left(\frac{o_i - p_i(a_j)}{\Delta o_i}\right)^2}, \tag{1}$$

SED
5, 2483–2507, 2013

Lithosphere and upper-mantle structure of the southern Baltic Sea

H. Steffen et al.

with n the number of observations, o_i the observed RSL, $p_i(a_j)$ the predicted RSL for a specific earth model a_j, and Δo_i the error of the observed RSL. The lowest value of χ relates to the best-fitting earth model a_b out of the 1089 provided. In addition, we analyze the model confidence within the observational errors by calculating the confidence parameter

$$\psi = \sqrt{\frac{1}{n}\sum_{i=1}^{n}\left(\frac{p_i(a_\mathrm{b}) - p_i(a_j)}{\Delta o_i}\right)^2}, \tag{2}$$

of the predicted RSL for the best-fitting earth model $p_i(a_\mathrm{b})$ to all other earth models. We show the 1σ- and 2σ-uncertainty for models that obey $\psi \leq 1$ and $1 < \psi \leq 2$, respectively, of the best-fitting earth model.

3.2 Ice models

We apply two different global ice models as load on the earth models. First, as in Steffen and Kaufmann (2005) and Vink et al. (2007), we use the model RSES provided by Kurt Lambeck (Research School of Earth Sciences, Australian National University) (see e.g. Lambeck et al., 1998). It combines the extent and the melting history from different separate ice models around the world. The other global ice model is the commonly used Ice-5G ice history (Peltier, 2004). Both RSES and Ice-5G belong to the type of ice models which are constrained by solid-earth models. Hence, best-fitting models usually tend to converge to a radial profile of specific lithospheric thickness and several viscosity layers as used in the ice-model generation. We exemplarily show the extent of the Fennoscandian ice sheet at Last Glacial Maximum of the two models in Fig. 2. There are distinct differences in collapse history, ice height and extent of the models, such as the bridge between Fennoscandia and the British Isles. The ice-sheet maximum can be spotted over the Gulf of Bothnia and central Sweden, with more ice in Ice-5G than RSES. Such differences between the ice models will consequently produce different patterns of rebound in the modeling.

SED
5, 2483–2507, 2013

4 Results

We start presenting the results with the discussion of the best-fitting three-layer earth models (Table 1) for each ice model and regional RSL dataset. Both ice models yield mainly similar earth structures for each region: A variation in lithospheric thickness from lower values along the Norwegian coast to higher values towards the Fennoscandian craton, and an increase in mantle viscosity from the upper to the lower mantle.

However, distinct differences can be found, when comparing the results for the two ice models: when focusing on the lithospheric thickness first, both the Oslo Graben as well as the German Baltic Sea coast is characterized by a 60 km thick lithosphere for both ice models. In between, the Fyn High has a higher thickness of 90 (RSES) to 100 km (Ice-5G). Southwestern Sweden reaches a higher thickness, however, here the values of the two ice models diverge with 90 km for Ice-5G and 130 km for RSES. Towards Poland the thickness increases up to 160 km for RSES, but only slightly to 100 km for Ice-5G. However, we note that the misfit for both ice models for the Polish data is much worse than for other areas.

Pronounced differences exist for the upper-mantle viscosity. While for Ice-5G only small variances between $[2–7] \times 10^{20}$ Pa s appear for the 5 investigated regions, the viscosity as determined with RSES varies by one order of magnitude with quite high upper-mantle viscosities of 2×10^{21} Pa s for southern Baltic Sea RSL data. Lower-mantle viscosity also shows a wide range of values, however, it has already been often noted that lower-mantle viscosity cannot be well determined with Fennoscandian RSL data due to their low resolving power to such great depths.

A closer look at the 1σ-range and the misfit maps (Fig. 3) shows that the lithospheric thickness and the upper-mantle viscosity in the Oslo Graben are quite well determined, while lower-mantle viscosity can be varied over a larger range, but would still give reasonable fits to the RSL data. In contrast, RSL data from SW Sweden highlight a larger variation of the three parameters. With the RSES ice model lithospheric thickness may range from 100 to 160 km and upper-mantle viscosity from $[3–10] \times 10^{20}$ Pa s. Using

SED
5, 2483–2507, 2013

Ice-5G, this range is smaller, but lithospheric thickness can also reach higher values, providing an overlap to possible thicknesses as determined with RSES.

For the Fyn High as well as the German Baltic Sea coast the 1σ-ranges become much narrower. Only lithospheric thickness as determined with RSES may be varied over almost the whole tested parameter range. These two datasets as well as SW Sweden show interesting features in the misfit maps of lithospheric thickness vs. upper-mantle viscosity. There are two regions of high misfits, one at about 10^{21} Pa s and thinner lithospheric thicknesses, and another one at about 10^{20} Pa s and lower covering the whole thickness range. This lower bound and the "island" at 10^{21} Pa s seem to force the best-fitting model to adopt upper-mantle viscosity values either of $[2–7] \times 10^{20}$ Pa s or of 2×10^{21} Pa s and larger. Lithospheric thickness is not strongly bounded. While Ice-5G prefers the lower viscosity area, RSES tends to higher viscosities. Although the 1σ-range for the RSES results does not cover the lower viscosity range, new deeper and older RSL data and an updated ice model may shift the results to similar values as determined with Ice-5G.

Another interesting behavior is that lower-mantle viscosity appears to be, except for SW Sweden, clearly determined. This also holds for the Polish data. Instead, the island at 10^{21} Pa s for upper-mantle viscosity does not appear. Small adjustments in lithospheric thickness may be possible.

5 Discussion

In the previous section we derived bounds for lithospheric thickness and upper- and lower-mantle viscosity for the different regions. We now take closer look at the fitted RSL data. While the locations Oslo Graben and SW Sweden are mainly near-field data with a large time and height/depth range, the other three regional subsets contain far-field data of younger age and smaller depth ranges, i.e. there is only a window of about 4000 yr where relative sea levels change by more than 30 m. Thus, it is challenging to identify the best-fitting modelled sea-level curve within the given error bars of the samples out of a large range of possible curves, despite the large number of samples within each subset. The determination of the best-fitting model can be much better achieved for Oslo Graben and SW Sweden. Here, we also note that the clear determination is much better for Oslo Graben as it contains a non-monotonic relative sea-level change with rising and falling sea levels. The low fit in Poland is additionally related to the low number of samples (31) in the database.

Further evaluation of our results is enabled by comparison of calculated sea-level curves from the best-fitting regional earth models to RSL data used. Figure 4 presents sea-level curves at 8 selected locations. In the Oslofjord and in western Sweden (HK, the archaeological data from Hensbacka culture sites), there is a very good fit between observations and the modelled curves. The RSL data from Limfjord in northern Denmark are not fitted well, but one has to note that there is only small variation of about 5 m in 5000 yr in this dataset, which is hard to trace for the model. Along the German Baltic Sea coast, this variation is much larger and thus better fits can be achieved. In Hiddensee both RSES and Ice-5G ice models result in a good match of the sea-level data. In the Oldenburger Graben and Redentin, the RSES ice model appears to trace the RSL data better, while in Körkwitz the Ice-5G ice model performs better. In Poland both ice models predict the sea-level rise well.

We can compare our results to a former investigation by Lambeck et al. (1998), where the authors already used Fennoscandian RSL data divided into several subregions. In the southwest, RSL data were grouped into three subsets: Oslo Fjord, SW Sweden and Denmark. This choice is similar to our study, but the Oslo Fjord dataset from Lambeck et al. (1998) did not contain RSL data from northern Denmark. For Oslofjord, the authors found a 80 km thick lithosphere and an upper-mantle viscosity of 1.5×10^{20} Pa s with an older version of the RSES ice model. In SW Sweden lithospheric thickness was with 50 km thickness 30 km thinner. Upper-mantle viscosity is here slightly higher having 2.5×10^{20} Pa s. Higher values were found in Denmark. Lithospheric thickness was determined with 150 km and upper-mantle viscosity with 4×10^{20} Pa s. While these results confirm the thicker lithosphere in Denmark/Fyn High

SED
5, 2483–2507, 2013

as well as the upper-mantle viscosities of our study, the differences in SW Sweden and the Oslofjord are large both in the lithospheric thickness estimate and also in the structural implications.

We therefore return to the lithosphere models derived from seismological data discussed in the introduction and visually compare them to our results. Figure 5 shows our results for the best lithospheric thickness estimates as colored maps, with the additional estimates from Steffen and Kaufmann (2005) for Fennoscandia and Vink et al. (2007) for the southern North Sea to give a more complete overview on GIA inferred lithospheric thickness. The results of Tesauro et al. (2009, A), Hamza et al. (2012, B) and Priestley and McKenzie (2013, C) are shown as contour lines. In the south and east of the area shown no results exist. The map is drawn in a simple manner by assigning the lithospheric thickness values of the best-fitting earth model for each region to the coordinates of each RSL data sample location.

In general, it becomes clear that a comparison of the seismically- and thermally-inferred lithospheric thickness values does not show a good match to our GIA-model results. The seismically- and thermally-inferred models all show lithospheric thicknesses of at least 110 km in the area under investigation. Also, their maximum values exceed 200 km considerably. However, we note that the three seismically- and thermally-inferred lithosphere models also do not show a good fit to each other either, except the general increase from west to east, and thus a thorough analysis and discussion is hampered.

The thickness according to Hamza et al. (2012) has a pronounced peak of 280 km in Poland and also shows decreasing values from east to west with no distinct change in the gradient except a kind of plateau with about 180 km in northwestern Denmark. Except the decrease in lithospheric thickness from east to west, there is no other further similar feature when compared to our GIA-modelling results.

The lithospheric thickness by Tesauro et al. (2009) reaches its highest value of 220 km in a broad band from southeastern Sweden to Latvia. It also shows decreasing values from east to west, however, the gradient is much steeper at the southwest-

SED
5, 2483–2507, 2013

ern Swedish coast. It becomes thinner to 150 km towards the northwest of Denmark, and then becoming thicker again. To the north and south of this area values drop to less than 110 km. There is a structural agreement in form of the east-west decrease. The Fyn High appears to lie further north in the thermal lithosphere. The thin GIA-lithosphere along the German Baltic Sea coast agrees to the plateau of 120 km in the thermal lithosphere. The structure of the Oslo Graben cannot be distinguished.

The best agreement of GIA-modelling-derived values is probably found in comparison to the new model by Priestley and McKenzie (2013). Both the EW-decrease trend and the location of the Fyn High fit structurally well. Small differences are found in the northwest of our investigation area and in the German Bight. However, we also have to note that the spatial resolution of this model is 2° and thus smaller features may not be clearly identified.

6 Conclusions

This is the first time that the regional earth structure in the southern Baltic Sea was determined with the help of regionally categorized RSL data and GIA modelling. Also, the lateral variation was visually compared to seismologically and/or thermally derived lithospheric thickness models for the first time. We therefore employed the software `ICEAGE` and two different global ice models. The lithospheric thickness varies from 60 km in the Oslo Graben and the German Baltic Sea coast to up to 160 km in Poland. We generally see a trend to thicker lithosphere from west to east. The Fyn High in between the Oslo Graben and Germany is at least 30 km thicker than the surrounding areas in the north and south. The variation in lithospheric thickness agrees to a certain extent, when compared visually, to thickness models based on seismological and/or thermal investigation. A perfect match in thickness is not possible.

Upper-mantle viscosity is about $[2–7] \times 10^{20}$ Pa s and thus confirms values found for Fennoscandia, the British Isles and the southern North Sea before. However, we note quite high values of 2×10^{21} Pa s for some regions when using the RSES ice history. As

SED
5, 2483–2507, 2013

this value seems to be unrealistic according to current knowledge, more RSL data need to be added and the ice model to be revised for this area. As expected, lower-mantle viscosity cannot be sufficiently determined.

Future investigations with hopefully more RSL data in the southern Baltic Sea and an updated ice model (both tested ice models experienced major improvements to date, but these revised versions have not been published yet) may help to further confirm the results herein and also overcome the differences between the results from the two ice models in certain areas.

Acknowledgements. We would like to thank Kurt Lambeck (Research School of Earth Sciences, Australian National University) and Magdala Tesauro (GFZ Potsdam) for kindly providing the RSES ice model and the thermal lithosphere model in Central and Southern Europe, respectively. Figures were prepared using GMT software (Wessel and Smith, 1998).

References

Artemieva, I. M.: The continental lithosphere: reconciling thermal, seismic, and petrologic data, Lithos, 109, 23–46, doi:10.1016/j.lithos.2008.09.015, 2009. 2487

Bennike, O., Jensen, J. B., Lemke, W., Kuijpers, A., and Lomholt, S.: Late- and post-glacial history of the Great Belt, Denmark, Boreas, 33, 18–33, doi:10.1111/j.1502-3885.2004.tb00993.x,2004. 2490

Bitinas, A., Damušyte, A., Hütt, G., Martma, T., Ruplenaite, G., Stančikaite, M., Ūsaityte, D., and Vaikmäe, R.: Stratigraphic correlation of Late Weichselian and Holocene Deposits in the Lithuanian coastal region, P. Est. Acad. Sci., 49, 200–217, 2000. 2489

Bitinas, A., Damušyte, A., Stančikaite, M., and Aleksa, P.: Geological development of the Nemunas River Delta and adjacent areas, West Lithuania, Geol. Q., 46, 375–389, 2002. 2489

Christensen, C., Fischer, A., and Mathiassen, D. R.: The great sea rise in the Storebælt, in: The Danish Storebælt Since the Ice Age – Man, Sea and Forest, edited by: Pedersen, L., Fischer, A., and Aaby, B., A/S Storebælt Fixed Link, Copenhagen, 45–54, 1997. 2489

Dziewonski, A. M. and Anderson D. L.: Preliminary reference Earth model, Phys. Earth Planet. In., 25, 297–356, doi:10.1016/0031-9201(81)90046-7, 1981. 2491

Eaton, D. W., Darbyshire, F., Evans, R. L., Grütter, H., Jones, A. G., and Yuan, X.: The elusive lithosphere-asthenosphere boundary (LAB) beneath cratons, Lithos, 109, 1–22, doi:10.1016/j.lithos.2008.05.009, 2009. 2487

Farrell, W. E. and Clark, J. A.: On postglacial sea level, Geophys. J. Roy. Astr. S., 46, 647–667, doi:10.1111/j.1365-246X.1976.tb01252.x, 1976. 2491

Geissler, W. H., Sodoudi, F., and Kind, R.: Thickness of the central and eastern european lithosphere as seen by S receiver functions, Geophys. J. Int., 181, 604–634, doi:10.1111/j.1365-246X.2010.04548.x, 2010. 2488

Gregersen, S., Voss, P., and the TOR Working Group: Summary of project TOR: delineation of a stepwise, sharp, deep lithosphere transition across Germany – Denmark – Sweden, Tectonophysics, 360, 61–73, doi:10.1016/S0040-1951(02)00347-5, 2002. 2487

Hamza, V. M. and Vieira, F. P.: Global distribution of the lithosphere-asthenosphere boundary: a new look, Solid Earth, 3, 199–212, doi:10.5194/se-3-199-2012, 2012. 2488, 2496, 2507

Hoffmann, G., Schmedemann, N., and Schafmeister, M.-T.: Relative sea-level curve for SE Rügen and Usedom Island (SW Baltic Sea coast, Germany) using decompacted profiles, Z. Dtsch. Ges. Geowiss., 160, 69–78, 2009. 2489

Hofmann, W. and Winn, K.: The Littorina transgression in the Western Baltic Sea as indicated by subfossil Chironomidae (Diptera) and Cladocera (Crustacea), Int. Rev. Hydrobiol., 85, 267–291, doi:10.1002/(SICI)1522-2632(200004)85:2/3<267::AID-IROH267>3.0.CO;2-Q, 2000. 2490

Jakobsen, O.: Die Grube-Wesseker Niederung (Oldenburger Graben, Ostholstein): Quartärgeologische und geoarchäologische Untersuchungen zur Landschaftsgeschichte vor dem Hintergrund des anhaltenden postglazialen Meeresspiegelanstiegs, Ph. D.-Thesis, Univerity Kiel, 190 pp., 2004. 2489

Kaufmann, G.: Program package ICEAGE, Version 2004, Manuscript, Institut für Geophysik der Universität Göttingen, 40 pp., 2004. 2491

Lambeck K., Smither, C., and Johnston, P.: Sea-level change, glacial rebound and mantle viscosity for northern Europe, Geophys. J. Int., 134, 102–144, doi:10.1046/j.1365-246x.1998.00541.x, 1998. 2488, 2492, 2495, 2504, 2506

Lampe, R., Meyer, H., Ziekur, R., Janke, W., and Endtmann, E.: Holocene evolution of an irregularly sinking coast and the interactions of sea-level rise, accumulation space and sediment supply, Bericht der Römisch-Germanischen Kommission 88, 15–46, 2007. 2489

Lampe, R., Endtmann, E., Janke, W., and Meyer, H.: Relative sea-level development and isostasy along the NE German Baltic Sea coast during the past 9 ka, E&G Quaternary Science Journal, 59, 3–20, doi:10.3285/eg.59.1-2.01, 2011. 2489

Lange, W. and Menke, B.: Beiträge zur frühpostglazialen erd- und vegetationsgeschichtlichen Entwicklung im Eidergebiet, insbesondere zur Flußgeschichte und zur Genese des sogenannten Basistorfes, Meyniana, 17, 29–44, 1967. 2489

Lidberg, M., Johansson, J. M., Scherneck, H.-G., and Milne, G. A.: Recent results based on continuous GPS observations of the GIA process in Fennoscandia from BIFROST, J. Geodyn., 50, 8–18, doi:10.1016/j.jog.2009.11.010, 2010. 2486

Lübke, H., Schmölcke, U., and Tauber, F.: Mesolithic hunter-fishers in a changing world: a case study of submerged sites on the Jäckelberg, Wismar Bay, northeastern Germany, in: Submerged Prehistory, edited by: Benjamin, J., Bonsall, C., Pickard, C., and Fischer, A., Oxbow Books, Oxford, 21–37, 2011. 2489

Mitrovica, J. X. and Milne, G. A.: Glaciation-induced perturbations in the Earth's rotation: a new appraisal, J. Geophys. Res., 103, 985–1005, doi:10.1029/97JB02121, 1998. 2491

Mitrovica, J. X., Davis, J. L., and Shapiro, I. I.: A spectral formalism for computing three–dimensional deformations due to surface loads 1. Theory, J. Geophys. Res., 99, 7057–7073, doi:10.1029/93JB03128, 1994. 2491

Peltier, W. R.: Global glacial isostasy and the surface of the iceage earth: the Ice-5G (VM2) model and GRACE, Annu. Rev. Earth Pl. Sc., 32, 111–149, doi:10.1146/annurev.earth.32.082503.144359, 2004. 2492, 2504, 2506

Priestley, K. and McKenzie, D.: The relationship between shear wave velocity, temperature, attenuation and viscosity in the shallow part of the mantle, Earth Planet. Sc. Lett., 381, 78–91, doi:10.1016/j.epsl.2013.08.022, 2013. 2488, 2496, 2497, 2507

Rößler, D., Moros, M., and Lemke, W.: The Littorina transgression in the southwestern Baltic Sea: new insights based on proxy methods and radiocarbon dating of sediment cores, Boreas, 40, 231–241, doi:10.1111/j.1502-3885.2010.00180.x, 2011. 2490

Schmitt, L., Larsson, S., Burdukiewicz, J., Ziker, J., Svedhage, K., Zamon, J., and Steffen, H.: Chronological insights, cultural change, and resource exploitation on the west coast of Sweden during the Late Paleolithic/early Mesolithic transition, Oxford J. Archaeol., 28, 1–27, doi:10.1111/j.1468-0092.2008.00317.x, 2009. 2490

Steffen, H. and Kaufmann, G.: Glacial isostatic adjustment of Scandinavia and northwestern Europe and the radial viscosity structure of the Earth's mantle, Geophys. J. Int., 163, 801–812, doi:10.1111/j.1365-246X.2005.02740.x, 2005. 2486, 2490, 2491, 2492, 2496

Steffen, H. and Wu, P.: Glacial isostatic adjustment in Fennoscandia – a review of data and modeling, J. Geodyn., 52, 169–204, doi:10.1016/j.jog.2011.03.002, 2011. 2485, 2486

Steffen, H., Wu, P., and Wang, H. S.: Determination of the Earth's structure in Fennoscandia from GRACE and implications on the optimal post-processing of GRACE data, Geophys. J. Int., 182, 1295–1310, doi:10.1111/j.1365-246X.2010.04718.x, 2010. 2491

Tauber, F.: Seafloor exploration with sidescan sonar for geo-archaeological investigations, Berichte der Römisch-Germanischen Kommission, 88, 67–79, 2007. 2489

Tesauro, M., Kaban, M. K., and Cloetingh, S. A. P. L.: A new thermal and rheological model of the European lithosphere, Tectonophysics, 476, 478–495, doi:10.1016/j.tecto.2009.07.022, 2009. 2487, 2488, 2496, 2507

Uścinowicz, S.: Relative sea level changes, glacio-isostatic rebound and shoreline displacement in the Southern Baltic, Polish Geological Institute Special Papers, 10, 1–80, 2003. 2489

Vink, A., Steffen, H., Reinhardt L., and Kaufmann, G.: Holocene relative sea-level change, isostatic subsidence and the radial viscosity structure of the mantle of north-western Europe (Belgium, the Netherlands, Germany, southern North Sea), Quaternary Sci. Rev., 26, 3249–3275, doi:10.1016/j.quascirev.2007.07.014, 2007. 2486, 2488, 2491, 2492, 2496

Wessel, P. and Smith, W. H. F.: New, improved version of generic mapping tools released, EOS T. Am. Geophys. Un., 79, 579, doi:10.1029/98EO00426, 1998. 2498

Winn, K., Averdieck, F.-R., Erlenkeuser, H., and Werner, F.: Holocene sea level rise in the western Baltic and the question of isostatic subsidence, Meyniana, 38, 61–80, 1986. 2489

Wu, P., Wang, H., and Steffen, H.: The role of thermal effect on mantle seismic anomalies under Laurentia and Fennoscandia from observations of Glacial Isostatic Adjustment, Geophys. J. Int., 192, 7–17, doi:10.1093/gji/ggs009, 2013. 2486

Yu, S.-Y., Berglund, B. E., Andrén, E., and Sandgren, P.: Mid-Holocene Baltic Sea transgression along the coast of Blekinge, SE Sweden – ancient lagoons correlated with beach ridges, GFF, 126, 257–272, doi:10.1080/11035890401263257, 2004. 2489

Table 1. Best-fitting three-layer 1-D earth models with RSES and Ice-5G ice load history, respectively, as derived for each regional RSL data subset. Values in brackets envelope σ_1-range for each model parameter. If no brackets appear, the σ_1-range envelopes the best-fitting model only. H_l lithospheric thickness, η_{UM} upper-mantle viscosity, η_{LM} lower-mantle viscosity, χ misfit.

Region	H_l in km	η_{UM} in 10^{20} Pa s	η_{LM} in 10^{22} Pa s	χ
		RSES		
SW Sweden	130 (100–160)	4 (3–10)	0.1 (0.1–1)	1.18
Oslo Graben	60 (60–70)	2	4 (0.4–10)	1.58
Fyn	90 (70–140)	20	10 (7–10)	3.88
German Baltic Sea	60 (60–150)	20	2 (2–3)	1.84
Polish Baltic Sea	160 (120–160)	20	10 (7–10)	5.70
		Ice-5G		
SW Sweden	90 (60–140)	2 (0.6–2)	0.1 (0.1–10)	0.87
Oslo Graben	60 (60–70)	2	0.4 (0.3–0.9)	2.19
Fyn	100 (90–110)	2	0.1	3.19
German Baltic Sea	60	4	4 (2–8)	1.95
Polish Baltic Sea	100 (90–100)	7	7	5.04

SED
5, 2483–2507, 2013

Lithosphere and upper-mantle structure of the southern Baltic Sea

H. Steffen et al.

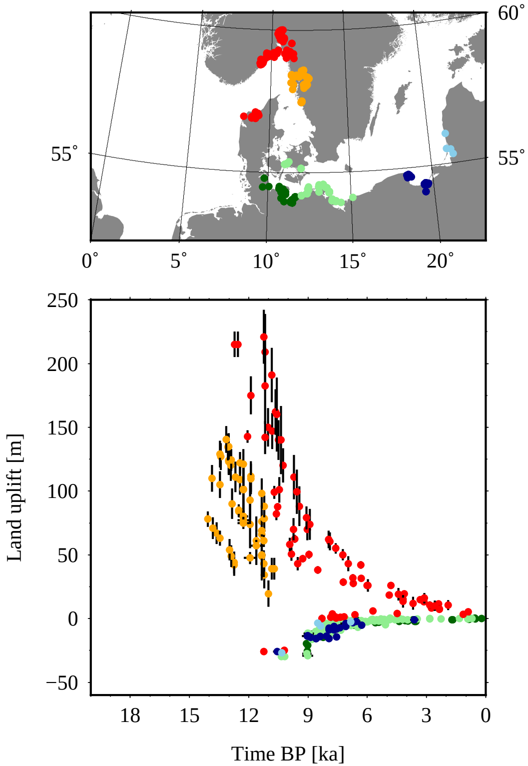

Fig. 1. Spatial and temporal distribution of relative sea-level data used in this study. Colors indicate regional subsets: Southwest Sweden (orange), Oslo Graben (red), Fyn High, Rügen Island and Darss Peninsula (light green), German Baltic Sea coast west of Darss Peninsula (dark green), Poland and Lithuania (dark and light blue), data uncertainties are indicated by vertical error bars.

SED
5, 2483–2507, 2013

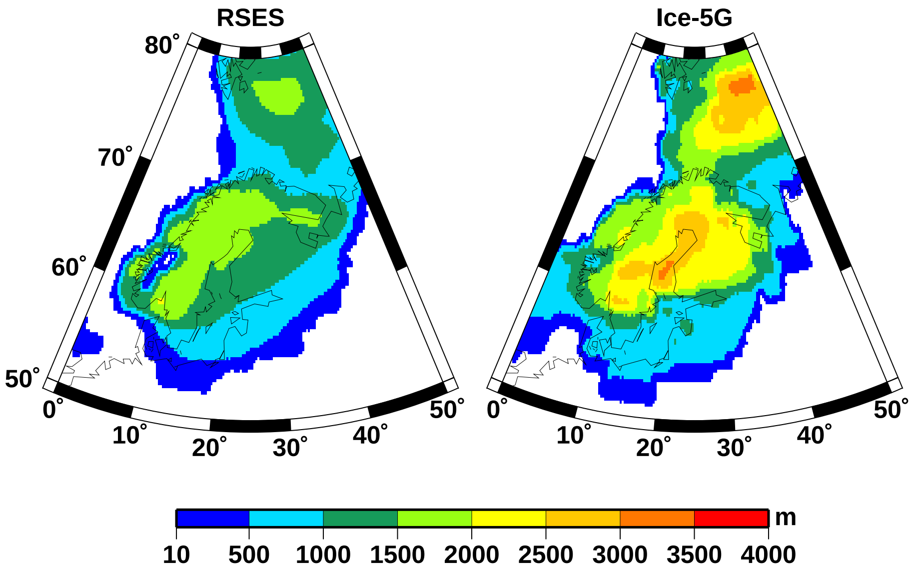

Fig. 2. Ice extent at Last Glacial Maximum in Fennoscandia from global ice models **(a)** RSES (Lambeck et al., 1998) and **(b)** Ice-5G (Peltier, 2004).

SED
5, 2483–2507, 2013

Lithosphere and upper-mantle structure of the southern Baltic Sea

H. Steffen et al.

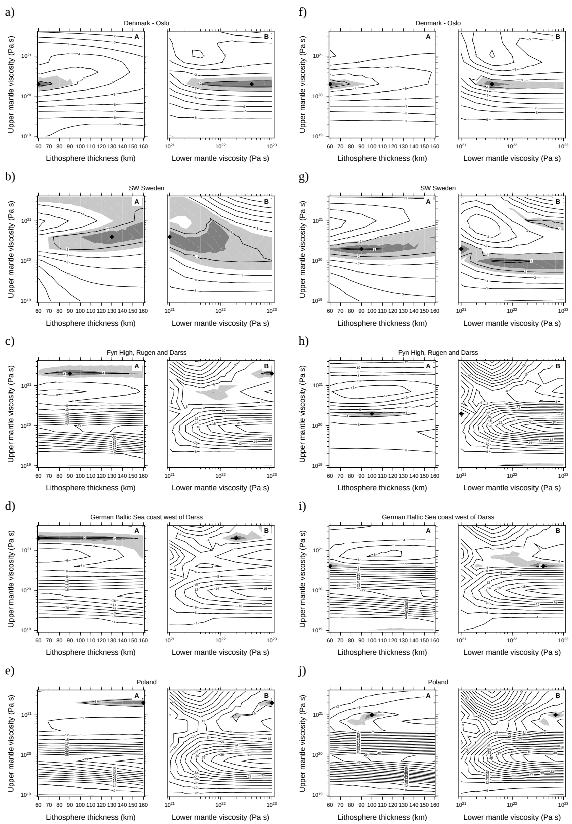

Fig. 3. Misfit for ice models RSES **(a–e)** and Ice-5G **(f–j)**, three-layer earth model and different datasets. **(A)** is the misfit map as a function of lithospheric thickness and upper-mantle viscosity for a fixed lower-mantle viscosity according to the best-fitting earth model, see Table 1. **(B)** is the misfit map as a function of upper and lower-mantle viscosities according to the best-fitting earth model for a fixed lithospheric thickness, see Table 1. **(a, f)** Misfit map for Oslo Graben RSL data. **(b, g)** Misfit map for SW-Sweden RSL data. **(c, h)** Misfit map for Fyn High data. **(d, i)** Misfit map for German Baltic Sea coast data. **(e, j)** Misfit map for Polish RSL data. The best 3-layer earth model is marked with a diamond, the light and dark shadings indicate the confidence regions $\psi \leq 1$ and $1 < \psi \leq 2$, respectively.

SED
5, 2483–2507, 2013

Lithosphere and upper-mantle structure of the southern Baltic Sea

H. Steffen et al.

Title Page
Abstract Introduction
Conclusions References
Tables Figures
◀ ▶
◀ ▶
Back Close
Full Screen / Esc
Printer-friendly Version
Interactive Discussion

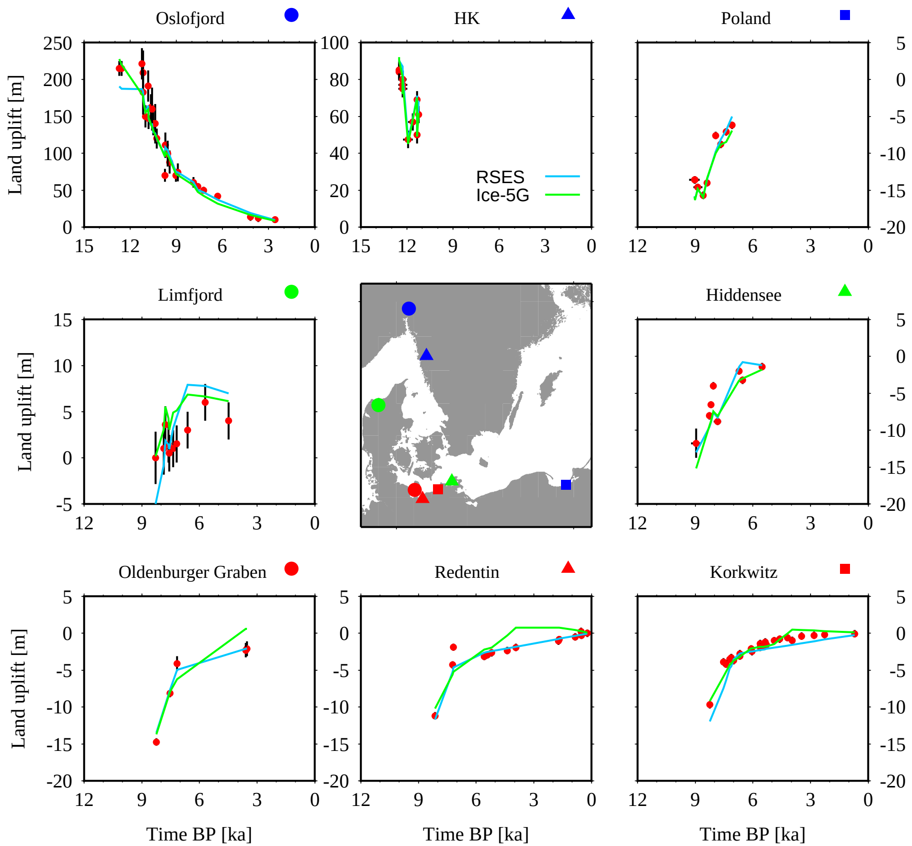

Fig. 4. Comparison of RSL data (red dots) at selected locations to sea-level curves as calculated with the best earth model for a respective region and ice model RSES (Lambeck et al., 1998, blue) and Ice-5G (Peltier, 2004, green).

SED
5, 2483–2507, 2013

Lithosphere and upper-mantle structure of the southern Baltic Sea

H. Steffen et al.

Title Page
Abstract | Introduction
Conclusions | References
Tables | Figures
◀| |▶
◀ ▶
Back | Close
Full Screen / Esc
Printer-friendly Version
Interactive Discussion

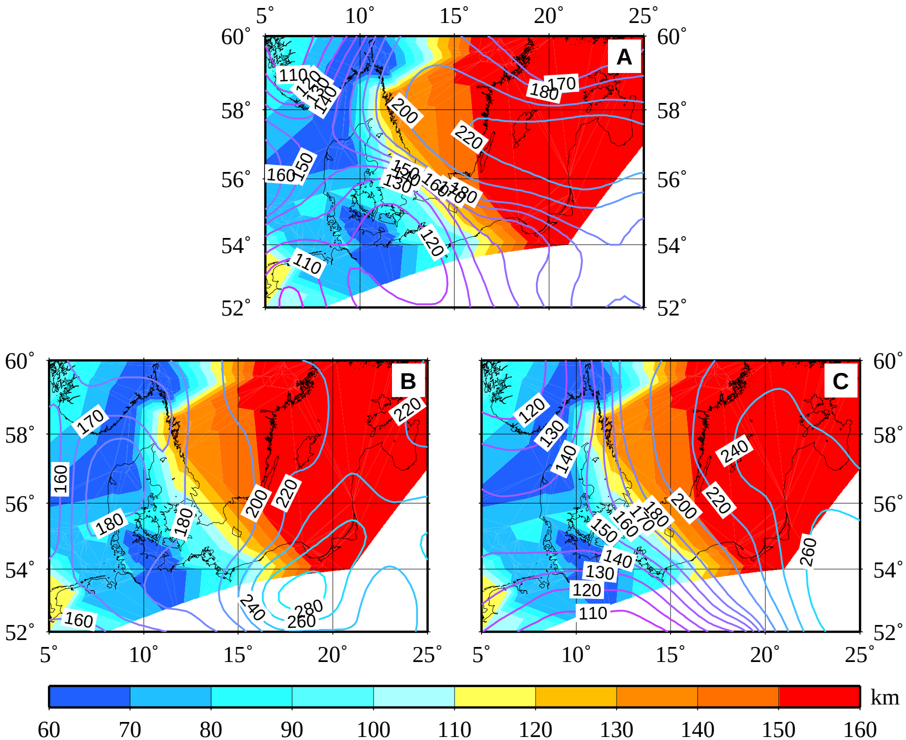

Fig. 5. Comparison of calculated regional lithospheric thickness variations (contour maps) to seismically- and thermally-derived lithospheric thicknesses (solid lines) by **(A)** Tesauro et al. (2009), **(B)** Hamza et al. (2012) and **(C)** Priestley and McKenzie (2013).

SED
5, 2483–2507, 2013